Initial Transcription by RNA Polymerase Proceeds Through a DNA-Scrunching Mechanism

Achillefs N. Kapanidis,[1,2]† Emmanuel Margeat,[1]* Sam On Ho,[1] Ekaterine Kortkhonjia,[1,3] Shimon Weiss,[1]† Richard H. Ebright[3]†

Using fluorescence resonance energy transfer to monitor distances within single molecules of abortively initiating transcription initiation complexes, we show that initial transcription proceeds through a "scrunching'' mechanism, in which RNA polymerase (RNAP) remains fixed on promoter DNA and pulls downstream DNA into itself and past its active center. We show further that putative alternative mechanisms for RNAP active-center translocation in initial transcription, involving "transient excursions" of RNAP relative to DNA or "inchworming" of RNAP relative to DNA, do not occur. The results support a model in which a stressed intermediate, with DNA-unwinding stress and DNA-compaction stress, is formed during initial transcription, and in which accumulated stress is used to drive breakage of interactions between RNAP and promoter DNA and between RNAP and initiation factors during promoter escape.

Transcription initiation is the first, and the most highly regulated, process in gene expression. In the first steps of transcription initiation, RNAP binds to promoter DNA and unwinds ~14 base pairs (bp) surrounding the transcription start site to yield a catalytically competent RNAP-promoter open complex (RP_o) (*1*–*3*). In subsequent steps of transcription initiation, RNAP enters into initial synthesis of RNA as an RNAP-promoter initial transcribing complex (RP_{itc}), typically engaging in abortive cycles of synthesis and release of short RNA products, and, on synthesis of an RNA product of ~9 to 11 nucleotides (nt), breaks its interactions with promoter DNA, breaks or weakens its interactions with initiation factors, leaves the promoter, and enters into processive synthesis of RNA as an RNAP-DNA elongation complex (RD_e) (*1*–*4*).

The mechanism by which the RNAP active center translocates relative to DNA in initial transcription has remained controversial. DNA-footprinting results indicated that, surprisingly, the upstream boundary of the promoter DNA segment protected by RNAP is unchanged in RP_{itc} as compared with RP_o (*5*–*7*). To reconcile the apparent absence of change in the upstream boundary of the promoter DNA segment protected by RNAP in RP_{itc} with the documented ability of RP_{itc} to synthesize RNA products up to ~9 to 11 nt in length, three models have been proposed (Fig. 1A) (*4*–*8*) [See also proposals for structurally unrelated single-subunit RNAP in (*9*–*15*).]

The first model, termed "transient excursions," invokes transient cycles of forward and reverse translocation of RNAP (Fig. 1A, top) (*5*). According to this model, in each cycle of abortive initiation, RNAP translocates forward as a unit, translocating 1 bp per phosphodiester bond formed [as in elongation; see (*16*)]; on release of the abortive RNA, RNAP reverse-translocates as a unit, regenerating the initial state. According to this model, the cycles of forward and reverse translocation are so short in duration and so infrequent in occurrence that, although they occur, they are not detected by a time-averaged, population-averaged method such as DNA-footprinting.

The second model, termed "inchworming," invokes a flexible element in RNAP (Fig. 1A, middle) (*6*, *7*). According to this model, in each cycle of abortive initiation, a module of RNAP containing the active center detaches from the remainder of RNAP and translocates downstream, translocating 1 bp per phosphodiester bond formed; on release of the abortive RNA, this module of RNAP retracts, regenerating the initial state.

The third model, termed "scrunching," invokes a flexible element in DNA (Fig. 1A, bottom) [(*4*, *5*, *8*); see also (*9*–*15*)]. According to this model, in each cycle of abortive initiation, RNAP pulls downstream DNA into itself, pulling in 1 bp per phosphodiester bond formed and accommodating the accumulated DNA as single-stranded bulges

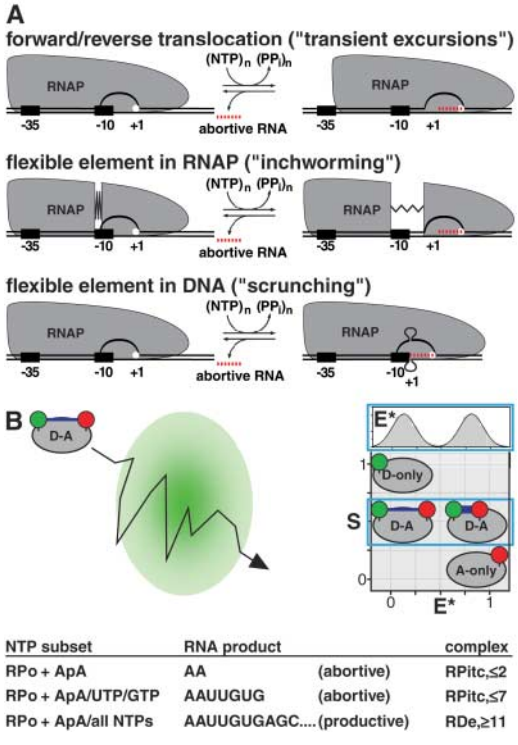

NTP subset	RNA product		complex
RPo + ApA	AA	(abortive)	$RPitc_{\leq 2}$
RPo + ApA/UTP/GTP	AAUUGUG	(abortive)	$RPitc_{\leq 7}$
RPo + ApA/all NTPs	AAUUGUGAGC....	(productive)	$RDe_{\geq 11}$

Fig. 1. Background and experimental approach. (**A**) Background. Three models have been proposed for RNAP active-center translocation during initial transcription [(*4*–*8*); see also (*9*–*15*)]: transient excursions, inchworming, and scrunching. White circles, RNAP active center; red dashed lines, RNA; black rectangles: promoter −10 and −35 elements. (**B**) Experimental approach. (Top) Use of confocal microscopy with ALEX (*19*–*21*) to monitor fluorescence of single transcription complexes. Single transcription complexes labeled with a fluorescent donor (D, green) and a fluorescent acceptor (A, red) diffuse through a femtoliter-scale observation volume (green oval; transit time ~1 ms); each molecule is illuminated with light that rapidly alternates between a wavelength that excites the donor and a wavelength that excites the acceptor. For each single molecule, and for each excitation wavelength, fluorescence emission is detected at both donor and acceptor emission wavelengths. This configuration permits calculation of two parameters: the donor-acceptor stoichiometry parameter, *S*, and the observed efficiency of the donor-acceptor energy transfer, *E** (*19*–*21*). The parameter *S* permits identification of molecules containing both donor and acceptor (*S* = 0.4 to 0.9; desired species; boxed in blue), molecules containing only a donor (*S* > 0.9; undesired species, arising from the presence of free σ^{70} molecules and buffer impurities), and molecules containing only an acceptor (*S* < 0.4; undesired species, arising from the dissociation of nonspecific complexes after heparin challenge). Subsequent analysis is performed only on molecules containing both donor and acceptor. (Bottom) Nucleoside triphosphate (NTP) subsets and corresponding RNA products and complexes.

[1]Department of Chemistry and Biochemistry and Department of Physiology, University of California, Los Angeles, CA 90095, USA. [2]Clarendon Laboratory, Department of Physics, and IRC in Bionanotechnology, University of Oxford, Oxford OX1 3PU, UK. [3]Howard Hughes Medical Institute, Department of Chemistry, and Waksman Institute, Rutgers University, Piscataway, NJ 08854, USA.

*Present address: Centre de Biochimie Structurale. CNRS UMR 5048. INSERM UMR 554. Université Montpellier I, 29 rue de Navacelles, 34090 Montpellier cedex, France.

†To whom correspondence should be addressed. E-mail: a.kapanidis1@physics.ox.ac.uk, sweiss@chem.ucla.edu, ebright@waksman.rutgers.edu

within the unwound region; on release of the abortive RNA, RNAP extrudes the accumulated DNA, which regenerates the initial state.

The three models are not necessarily mutually exclusive; in principle, combinations of mechanisms may be used, or different mechanisms may be used at different stages of initial synthesis (e.g., one for synthesis of short RNA products, and another for synthesis of longer RNA products).

In this work, we have directly tested the predictions of the three models in Fig. 1A by monitoring distances within single molecules of RP_o and RP_{itc} (*17*). We used fluorescence resonance energy transfer (FRET) (*18*) to monitor distances between fluorescent donors and acceptors incorporated at specific sites within RNAP and DNA. We used confocal optical microscopy with alternating-laser excitation (ALEX) (*19*–*21*) to detect and to quantify fluorescence of single molecules in solution transiting a femtoliter-scale observation volume (Fig. 1B, top left). For each such single molecule, we extracted the donor-acceptor stoichiometry parameter, *S*, and the observed efficiency of donor-acceptor energy transfer, *E** (Fig. 1B, top right). We analyzed *Escherichia coli* RNAP holoenzyme (RNAP core in complex with the initiation factor σ^{70}) (*1*–*3*) and a consensus *E. coli* promoter (*lac*CONS) (*22*) (fig. S1).

We performed four sets of experiments to assess the following: (i) movement of the RNAP leading edge relative to DNA; (ii) movement of the RNAP trailing edge relative to DNA; (iii) expansion and contraction of RNAP; and (iv) expansion and contraction of DNA. In each case, we performed measurements with RP_o containing the initiating dinucleotide ApA [RP_o + ApA, referred to hereafter as RP_o (Fig. 1B, bottom)] and with RP_{itc} engaged in iterative abortive synthesis of RNA products up to 7 nt in length [$RP_{itc,\leq 7}$; prepared by addition of UTP and GTP to RP_o (Fig. 1B, bottom)].

To assess possible movement of the RNAP leading edge relative to downstream DNA in initial transcription, we monitored FRET between a fluorescent donor incorporated at the RNAP leading edge (σ^{70} residue 366, located in σR2, the σ^{70} domain responsible for recognition of the promoter –10 element) and a fluorescent acceptor incorporated at a site in downstream DNA (position +20) (Fig. 2A). The results indicated that, on transition from RP_o to $RP_{itc,\leq 7}$, the mean observed efficiency *E** significantly increases, which implies that the mean donor-acceptor distance, *R*, significantly decreases (Fig. 2A, right). The quantitative increase in mean *E** corresponds to a decrease in mean *R* of ~7 Å (Fig. 2A, right; table S1). Parallel experiments performed using a donor incorporated at a different site at the RNAP leading edge (σ^{70} residue 396, also located in σR2), or using an acceptor incorporated at a different site in downstream DNA (position +15 or position +25), also showed decreases in mean donor-acceptor distance [decreases of ~5 to ~16 Å (fig. S2)]. Control experiments performed in the presence of rifampicin, an inhibitor that blocks synthesis of RNA products >2 nt in length (*23*), showed that the observed decreases in mean donor-acceptor distance required synthesis of RNA products >2 nt in length (fig. S3). We infer that the RNAP leading edge translocates relative to downstream DNA in initial transcription. Furthermore, we infer that, during initial transcription with these reagents and reaction conditions, complexes predominantly occupy states in which the RNAP leading edge is translocated relative to downstream DNA, not states in which the RNAP leading edge is positioned as in RP_o. This implies that the rate-limiting step in initial transcription with these reagents and reaction conditions is abortive-product release and RNAP active-center reverse-translocation [see also (*24*)]. The finding that the RNAP leading edge translocates relative to downstream DNA is consistent with the predictions of all three models for initial transcription (Figs. 1A and 2A). The finding that RNAP predominantly occupies states in which the RNAP leading edge is translocated is incompatible with, or at least problematic for, the transient-excursion model, which invokes translocated states that are short in duration and infrequent in occurrence.

To assess possible movement of the RNAP trailing edge relative to upstream DNA in initial transcription, we monitored FRET between a fluorescent donor incorporated at the RNAP trailing edge (σ^{70} residue 569, located in σR4, the σ^{70} domain responsible for recognition of the

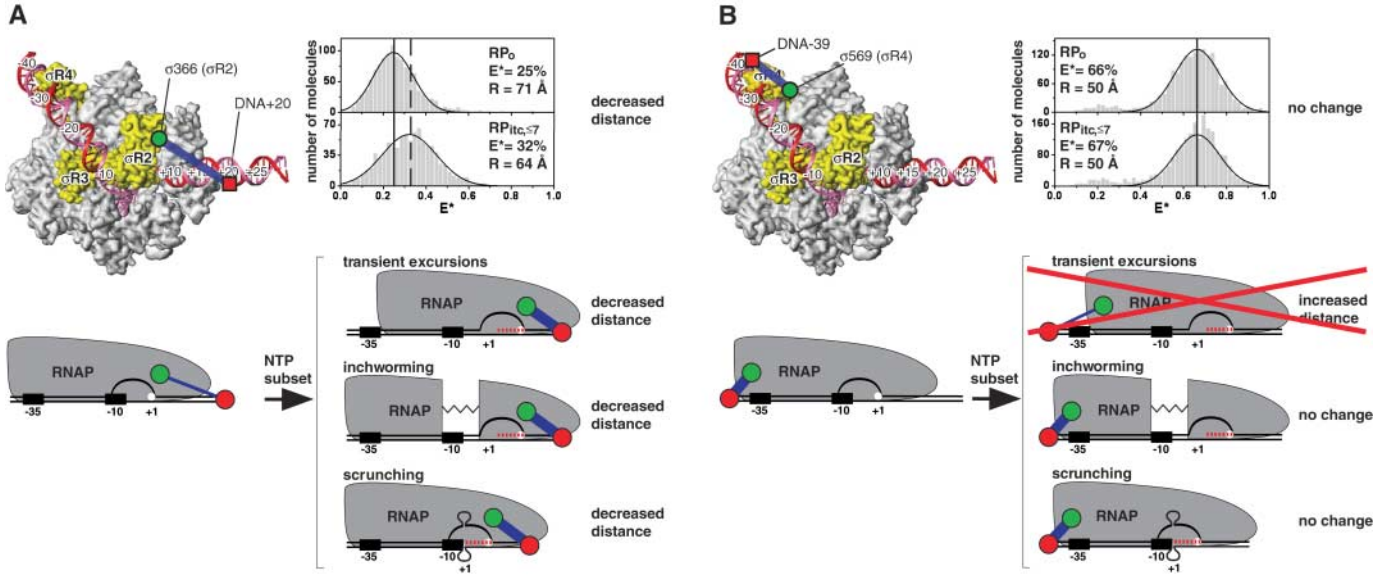

Fig. 2. Initial transcription does not involve transient excursions. (**A**) Experiment documenting movement of the RNAP leading edge relative to downstream DNA [tetramethylrhodamine as donor at σ^{70} residue 366 (located in σR2, the σ^{70} domain responsible for recognition of the promoter –10 element); Cy5 as acceptor at DNA position +20]. (Top left) Structural model of RP_o (*28*) showing positions of donor (green circle) and acceptor (red square). RNAP core is in gray; σ^{70} is in yellow; the DNA template and nontemplate strands are in red and pink, respectively. (Top right) *E** histograms for RP_o and $RP_{itc,\leq 7}$. The vertical line and vertical dashed line mark mean *E** values for RP_o and $RP_{itc,\leq 7}$, respectively. (Bottom) Predictions of the three models. (**B**) Experiment documenting absence of movement of the RNAP trailing edge relative to downstream DNA [tetramethylrhodamine as donor at σ^{70} residue 569 (located in σR4, the σ^{70} domain responsible for recognition of the promoter –35 element); Cy5 as acceptor at DNA position –39]. Subpanels as in (A).

promoter –35 element) and a fluorescent acceptor incorporated at a site in upstream DNA (position –39) (Fig. 2B). In this case, the results indicated that, on transition from RP_o to $RP_{itc,\leq 7}$, mean E^* remains unchanged (Fig. 2B, top right), which implies that the mean donor-acceptor distance remains unchanged. Parallel experiments performed using a donor incorporated at a different site at the RNAP trailing edge (σ^{70} residue 596, also located in σR4) also imply that the mean donor-acceptor distance remains unchanged (fig. S4). Control experiments showed that our probe sites are well positioned to detect a translocation-dependent change in mean donor-acceptor distance and would detect a change if it occurred (fig. S5). We infer that the RNAP trailing edge does not translocate relative to upstream DNA in initial transcription. Specifically, we infer that the σ^{70} domain that interacts with promoter –35 element does not alter its interactions with DNA in initial transcription. This is true even for reaction conditions where it can be shown that the RNAP leading edge translocates relative to downstream DNA (Fig. 2A). These findings are inconsistent with the fundamental prediction of the transient-excursions model; that is, any molecule having the RNAP leading edge translocated relative to DNA also must have the RNAP trailing edge translocated relative to DNA (Figs. 1A and 2B). We conclude that initial transcription does not involve transient excursions.

To assess possible expansion and contraction of RNAP in initial transcription, we first monitored FRET between a fluorescent donor incorporated at the RNAP leading edge (σ^{70} residue 366, located in σR2, and shown in Fig. 2A to translocate relative to downstream DNA) and a fluorescent acceptor incorporated at a site in –10/–35 spacer DNA (position –20)

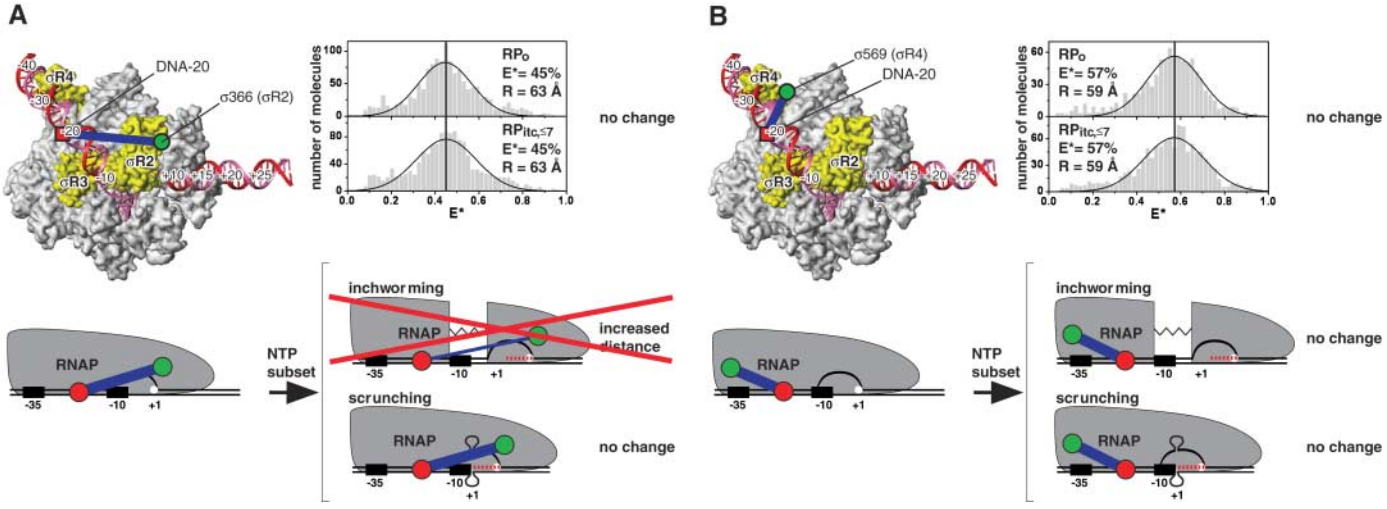

Fig. 3. Initial transcription does not involve inchworming. (**A**) Experiment documenting absence of movement of the RNAP leading edge relative to –10/–35 spacer DNA [tetramethylrhodamine as donor at σ^{70} residue 366 (located in σR2, the σ^{70} domain responsible for recognition of the promoter –10 element); Alexa647 as acceptor at DNA position –20]. Subpanels as in Fig. 2A. (**B**) Experiment documenting absence of movement of the RNAP trailing edge relative to –10/–35 spacer DNA [tetramethylrhodamine as donor at σ^{70} residue 569 (located in σR4, the σ^{70} domain responsible for recognition of the promoter –35 element); Alexa647 as acceptor at DNA position –20]. Subpanels as in Fig. 2A.

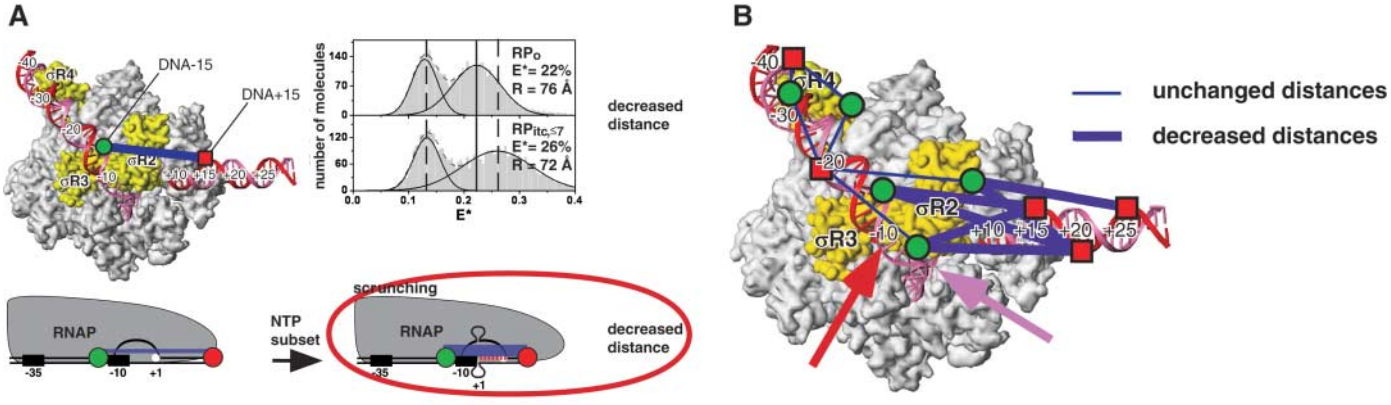

Fig. 4. Initial transcription involves scrunching. (**A**) Experiment documenting contraction of DNA between positions –15 and +15 [Cy3B as donor at DNA position –15; Alexa647 as acceptor at DNA position +15]. Subpanels as in Fig. 2A. [The two donor-acceptor species in the E^* histograms comprise free DNA (lower-E^* species) and RP_o or $RP_{itc,\leq 7}$ (higher-E^* species; higher FRET attributable to RNAP-induced DNA bending)]. Free DNA is present in all experiments, arising from dissociation of nonspecific complexes after heparin challenge during preparation of RP_o, but is detected only in this experiment, because DNA contains both donor and acceptor only in this experiment. (**B**) Summary of results. Structural model of RP_o (*28*) showing all donor-acceptor distances monitored in this work (Figs. 2 to 4A and figs. S2 to S8). Distances that remain unchanged on transition from RP_o to $RP_{itc,\leq 7}$ are indicated with thin blue lines. Distances that decrease on transition from RP_o to $RP_{itc,\leq 7}$ are indicated with thick blue lines. The red and pink arrows show the proposed positions at which scrunched template-strand DNA and scrunched nontemplate-strand DNA, respectively, emerge from RNAP (i.e., near template-strand positions –9 to –10 and near nontemplate-strand positions –5 to –6).

(Fig. 3A). In this case, the results indicated that, on transition from RP_o to $RP_{itc,\leq 7}$, mean E^* remains unchanged (Fig. 3A, top right), which implies that the mean donor-acceptor distance remains unchanged. Parallel experiments performed using a donor incorporated at a different site at the RNAP leading edge [σ^{70} residue 396, also located in σR2, and also shown (in fig. S2) to translocate relative to downstream DNA] also imply that the mean donor-acceptor distance remains unchanged (fig. S6). We next monitored FRET between a fluorescent donor incorporated at the RNAP trailing edge (σ^{70} residue 569 or σ^{70} residue 596, located in σR4) and a fluorescent acceptor incorporated at a site in the –10/–35 spacer DNA (position –20) (Fig. 3B and fig. S6). In this case also, the results indicated that, on transition from RP_o to $RP_{itc,\leq 7}$, mean E^* remains unchanged (Fig. 3B and fig. S6), which implies that the mean donor-acceptor distance remains unchanged. We infer that RNAP does not expand or contract in initial transcription. Furthermore, we infer that the leading edge of RNAP does not translocate relative to DNA upstream of the unwound region—even under reaction conditions where we have shown that the RNAP leading edge translocates relative to downstream DNA (Fig. 2A). These findings are inconsistent with the fundamental prediction of the inchworming model: namely, any molecule having the RNAP leading edge translocated relative to downstream DNA also must have the RNAP leading edge translocated relative to DNA upstream of the unwound region (Figs. 1A and 3A). We conclude that initial transcription does not involve inchworming.

To assess possible expansion and contraction of DNA in initial transcription, we monitored FRET between a fluorescent donor incorporated at a site in –10/–35 spacer DNA (position –15) and a fluorescent acceptor incorporated at a site in downstream DNA (position +15) (Fig. 4A). The results indicated that, upon transition from RP_o to $RP_{itc,\leq 7}$, mean E^* significantly increases (Fig. 4A, top right), which implies that the mean donor-acceptor distance, mean R, significantly decreases. The quantitative increase in mean E^* corresponds to a decrease in mean R of ~4 Å (Fig. 4A, top right). Additional experiments performed using an acceptor incorporated at a different site in downstream DNA (position +20) also showed a decrease in mean donor-acceptor distance (decrease of ~6 Å; fig. S7). Control experiments performed in the presence of rifampicin showed that the observed decreases in mean donor-acceptor distance required synthesis of an RNA product >2 nt in length (fig. S8). We infer that the DNA segment between –10/–35 spacer DNA and downstream DNA contracts in initial transcription. These findings document the fundamental prediction of the simplest version of the scrunching model; that is, any molecule having the RNAP leading edge translocated relative to downstream DNA also must have contraction—scrunching—of the DNA segment between –10/–35 spacer DNA and downstream DNA (Figs. 1A and 4A). We conclude that initial transcription involves scrunching.

We note that all measured distances between RNAP and upstream DNA or –10/–35 spacer DNA remain unchanged on transition from RP_o to $RP_{itc,\leq 7}$, (Fig. 4B, thin blue lines), whereas all measured distances between RNAP and downstream DNA, or between the –10/–35 spacer and downstream DNA, decrease on transition from RP_o to $RP_{itc,\leq 7}$, (Fig. 4B, thick blue lines). We infer that DNA scrunching occurs exclusively within the DNA segment comprising positions –15 to +15. This DNA segment contains the unwound region ("transcription bubble") and, in structural models of RP_o (*22*, *25*–*28*), is located within and immediately upstream of the RNAP active-center cleft. Inspection of structural models of RP_o and RD_e (*22*, *25*–*29*) indicates that there is insufficient space within the RNAP active-center cleft to accommodate scrunched DNA and that scrunched DNA instead must emerge from RNAP into bulk solvent immediately upstream of the RNAP active-center cleft. Although the locations at which scrunched DNA emerges are not known, we propose that the scrunched template DNA strand and nontemplate DNA strand emerge at or near the points where the respective DNA strands normally emerge from RNAP immediately upstream of the RNAP active-center cleft; that is, at or near positions –9 to –10 of the template strand and positions –5 to –6 of the nontemplate strand (Fig. 4B, red and pink arrows).

The results in this paper and in the companion paper (*30*) establish that initial transcription involves DNA scrunching. In contrast, processive transcription elongation involves simple translocation, not DNA scrunching [(*16*); see also (*19*)]. Thus, there is a fundamental difference in the mechanisms of RNAP active-center translocation in initial transcription and processive transcription elongation.

The results in this paper and in the companion paper (*30*) provide strong support for existence of a "stressed intermediate" in initial transcription (*4*, *6*), specifically a stressed intermediate with accumulated DNA-scrunching stress (DNA-unwinding stress and DNA-compaction stress). We postulate that the accumulated DNA-scrunching stress in the stressed intermediate provides the driving force for abortive initiation and also provides the driving force for promoter escape and productive initiation. Thus, we postulate that the accumulated DNA-scrunching stress in the stressed intermediate can be resolved in two ways: either (i) by releasing the RNA product, retaining interactions with promoter DNA, retaining interactions with initiation factors, retaining an unchanged position of the RNAP trailing edge, extruding scrunched DNA, and re-forming RP_o (abortive initiation); or (ii) by retaining the RNA product, breaking interactions with promoter DNA, breaking interactions with initiation factors, translocating the RNAP trailing edge, and forming RD_e (promoter escape and productive initiation).

References and Notes

1. M. T. Record Jr., W. S. Reznikoff, M. L. Craig, K. L. McQuade, P. J. Schlax, in Escherichia coli *and* Salmonella typhimurium: *Cellular and Molecular Biology*, F. C. Neidhardt *et al.*, Eds. (ASM Press, Washington, DC, 1996), vol. 1, pp. 792–820.
2. B. A. Young, T. M. Gruber, C. A. Gross, *Cell* **109**, 417 (2002).
3. K. S. Murakami, S. A. Darst, *Curr. Opin. Struct. Biol.* **13**, 31 (2003).
4. L. M. Hsu, *Biochim. Biophys. Acta* **1577**, 191 (2002).
5. A. J. Carpousis, J. D. Gralla, *J. Mol. Biol.* **183**, 165 (1985).
6. D. C. Straney, D. M. Crothers, *J. Mol. Biol.* **193**, 267 (1987).
7. B. Krummel, M. J. Chamberlin, *Biochemistry* **28**, 7829 (1989).
8. M. Pal, A. S. Ponticelli, D. S. Luse, *Mol. Cell* **19**, 101 (2005).
9. G. M. Cheetham, D. Jeruzalmi, T. A. Steitz, *Nature* **399**, 80 (1999).
10. G. M. Cheetham, T. A. Steitz, *Science* **286**, 2305 (1999).
11. L. G. Brieba, R. Sousa, *EMBO J.* **20**, 6826 (2001).
12. M. Jiang, M. Rong, C. Martin, W. T. McAllister, *J. Mol. Biol.* **310**, 509 (2001).
13. C. Liu, C. T. Martin, *J. Mol. Biol.* **308**, 465 (2001).
14. E. A. Esposito, C. T. Martin, *J. Biol. Chem.* **279**, 44270 (2004).
15. P. Gong, E. A. Esposito, C. T. Martin, *J. Biol. Chem.* **279**, 44277 (2004).
16. E. A. Abbondanzieri, W. J. Greenleaf, J. W. Shaevitz, R. Landick, S. M. Block, *Nature* **438**, 460 (2005).
17. Materials and methods are available as supporting online material on *Science* Online.
18. P. R. Selvin, *Nat. Struct. Biol.* **7**, 730 (2000).
19. A. N. Kapanidis *et al.*, *Proc. Natl. Acad. Sci. U.S.A.* **101**, 8936 (2004).
20. A. N. Kapanidis *et al.*, *Mol. Cell* **20**, 347 (2005).
21. N. K. Lee *et al.*, *Biophys. J.* **88**, 2939 (2005).
22. V. Mekler *et al.*, *Cell* **108**, 599 (2002).
23. E. A. Campbell *et al.*, *Cell* **104**, 901 (2001).
24. E. Margeat *et al.*, *Biophys. J.* **90**, 1419 (2005).
25. N. Naryshkin, A. Revyakin, Y. Kim, V. Mekler, R. H. Ebright, *Cell* **101**, 601 (2000).
26. K. S. Murakami, S. Masuda, E. A. Campbell, O. Muzzin, S. A. Darst, *Science* **296**, 1285 (2002).
27. D. G. Vassylyev *et al.*, *Nature* **417**, 712 (2002).
28. C. L. Lawson *et al.*, *Curr. Opin. Struct. Biol.* **14**, 10 (2004).
29. N. Korzheva *et al.*, *Science* **289**, 619 (2000).
30. A. Revyakin, C. Liu, R. H. Ebright, T. R. Strick, *Science* **314**, 1139 (2006).

31. We thank X. Michalet for discussions, and J. Tang and Y. Wang for assistance. This work was funded by NIH grant GM069709-01 to S.W. and A.N.K., U.S. Department of Energy grants 02ER63339 and 04ER63938 to S.W., and NIH grant GM41376 and a Howard Hughes Medical Institute Investigatorship to R.H.E.

Supporting Online Material

www.sciencemag.org/cgi/content/full/314/5802/1144/DC1
Materials and Methods
Figs. S1 to S8
Table S1
References

16 June 2006; accepted 28 September 2006
10.1126/science.1131399